Dispersion Characteristics of Open Microstrip Lines

MASANORI KOBAYASHI, MEMBER, IEEE, AND FUMIHIRO ANDO

Abstract—**A method based on spectral-domain analysis is derived to compute effectively and automatically the effective relative permittivity of an open microstrip line. Simple but accurate closed-form expressions are used as the basis functions of the longitudinal and transverse current distributions. The numerical results are shown in tables and figures for various cases and compared with other available results. The results presented here are seen as having a high degree of accuracy and may be used as reference standards.**

I. Introduction

ACCURATE CALCULATION of the dispersion characteristics of open microstrip lines can be carried out by hybrid-mode analysis. This dispersion analysis has been studied by a number of researchers and by various methods (see [1]–[7] and references therein). These methods are intrinsically rigorous, but need long computation times since the longitudinal and transverse current distributions must be expressed using a large number of basis functions to calculate the dispersion characteristics numerically with a high degree of accuracy. The results in many papers were calculated with a small number of basis functions to save computation time, and the current distributions were not expressed accurately. This is the major cause for the significant discrepancies between many computed results, as shown by Kuester and Chang [5, fig. 2] and by Fig. 3 in the present paper.

An attempt is required at present to confirm which numerical results are more "exact" and particularly to show results with a high degree of accuracy for use as a "standard."

In the spectral-domain analysis with powerful features proposed by Itoh and Mittra [4], the choice of the basis functions is important for numerical efficiency. One of the present authors proposed simple but accurate closed-form expressions for the normalized longitudinal and transverse current distributions on microstrip [13].[1]

In this paper, using these expressions the frequency-dependent characteristics for the effective relative permittivities of microstrip lines are calculated accurately by spectral-domain analysis [4]. In the numerical calculation, a method is derived to determine effectively and automatically the effective relative permittivity $\epsilon_{\text{eff}}^{*}(f)$ using only one trial value, and the computation time is greatly reduced. The numerical results are shown in tables and figures for the cases of various shape ratios and various relative permittivities of the substrate.

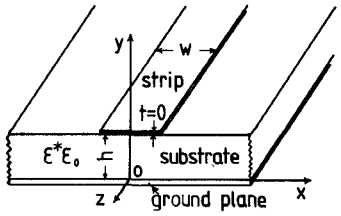

Fig. 1. Microstrip configuration.

II. Calculating Method

Fig. 1 shows the open microstrip line structure, assumed to be uniform and infinite in both x- and z-directions. The infinitely thin strip and the ground plane are perfect conductors. It is also assumed that the substrate material is lossless and its relative permittivity and permeability are ϵ^* and $\mu^*(=1)$, respectively. It is advantageous to carry out the investigation with functions that are Fourier transformed with respect to the x-axis. For convenience, the Fourier transform of a variable with respect to x is denoted by a tilde (~) above it, such as

$$\tilde{f}(\alpha) = \int_{-\infty}^{\infty} f(x) e^{+j\alpha x}\, dx. \tag{1}$$

This definition is the same as that given by Itoh and Mittra [4]. Propagation in the z-direction according to $\exp(-j\beta z)$ and time dependence of $\exp(j\omega t)$ are assumed, where β is the unknown propagation constant and ω is the operating angular frequency.

The unknown current components on the strip are denoted by $\tilde{I}_x(\alpha)$ and $\tilde{I}_z(\alpha)$, respectively. According to Itoh and Mittra [4], we can solve the boundary value problem in the spectral domain for the following boundary conditions at the interface between the substrate (region 1) and the air (region 2):

$$\tilde{E}_{x1}(\alpha, h) = \tilde{E}_{x2}(\alpha, h) \tag{2a}$$

$$\tilde{E}_{z1}(\alpha, h) = \tilde{E}_{z2}(\alpha, h) \tag{2b}$$

$$\tilde{H}_{z1}(\alpha, h) - \tilde{H}_{z2}(\alpha, h) = -\tilde{I}_x(\alpha) \tag{3a}$$

$$\tilde{H}_{x1}(\alpha, h) - \tilde{H}_{x2}(\alpha, h) = \tilde{I}_z(\alpha). \tag{3b}$$

Manuscript received April 4, 1986, revised September 10, 1986.

The authors are with the Department of Electrical Engineering, Faculty of Engineering, Ibaraki University, 4-12-1 Nakanarusawa-Machi, Hitachi, Ibaraki, Japan.

IEEE Log Number 8611622.

[1]Main corrections in [13]: longitudinal → transverse in figs. 8–10; $i_x(x_m)v(f)/(i_z(0)\omega)(m) \rightarrow ji_x(x_m)v(f)/(i_z(0)\omega h)$ in fig. 11.

However misprints exist in the equations given in [4], and the following corrections should be made: $\tilde{J}_x(\alpha)$ in (4a) and (4b) $\rightarrow -\tilde{J}_x(\alpha)$, and det in the equations for G_{11} and $G_{22} \rightarrow -\det$.

After these corrections, expanding the unknown current components $\tilde{I}_x(\alpha)$ and $\tilde{I}_z(\alpha)$ in terms of the known basis functions $\tilde{I}_{xn}(\alpha)$ and $\tilde{I}_{zn}(\alpha)$ as

$$\tilde{I}_x(\alpha) = \sum_{n=1}^{M} c_n \tilde{I}_{xn}(\alpha) \tag{4a}$$

$$\tilde{I}_z(\alpha) = \sum_{n=1}^{N} d_n \tilde{I}_{zn}(\alpha) \tag{4b}$$

and using the method given in [4], we can obtain the integral simultaneous equations [4, eq. (10)].

The propagation constant β can be solved by setting the determinant of [4, eq. (10)] equal to zero and seeking the root of the resulting equation. However, each numerical computation of the integrations [4, eq. (11)] intrinsically needs a long computation time so that the total computation time becomes longer if the current components (4a), (4b) are expanded in terms of a number of basis functions.

To avoid this, we can use the simple but accurate closed-form expressions of the normalized current distributions proposed in the previous paper [13] as follows:

$$I_{x1}(x) = \begin{cases} 1-\left(1-\dfrac{x}{x_m}\right)^{\nu}, & 0 \leqslant x \leqslant x_m \\ \sqrt{1-\left(\dfrac{x-x_m}{\frac{w}{2}-x_m}\right)^2}, & x_m \leqslant x \leqslant \dfrac{w}{2} \end{cases} \tag{5a}$$

$$I_{x1}(-x) = -I_{x1}(x)$$

$$\nu = \begin{cases} 1.6, & \dfrac{w}{h} < 7 \\ 1.5, & 7 \leqslant \dfrac{w}{h} \end{cases}$$

and

$$I_{z1}(x) = 1 + 10\left(1-\frac{2x_c}{w}\right)\frac{M(x)-1}{M(x_c)-1} \tag{5b}$$

$$M(x) = 1/\sqrt{1-(2x/w)^2}. \tag{6}$$

The values $2x_m/w$ and $2x_c/w$ depend strongly on the shape ratio w/h and can be found in the previous paper [13, figs. 5 and 10]. These closed-form expressions satisfy the edge singularities [8].

Using these as the basis functions, we can express the current components $\tilde{I}_x(\alpha)$ and $\tilde{I}_z(\alpha)$ in (4) as

$$\tilde{I}_x(\alpha) = c_1 \tilde{I}_{x1}(\alpha) \tag{7a}$$

$$\tilde{I}_z(\alpha) = d_1 \tilde{I}_{z1}(\alpha) \tag{7b}$$

where

$$\begin{aligned} \tilde{I}_{x1}(\alpha) = 2j\Bigg[& -\frac{\cos \alpha x_m}{\alpha} + \frac{\pi}{2\alpha}\left\{(\cos \alpha x_m) H_1\left(\alpha\left(\frac{w}{2}-x_m\right)\right)\right. \\ & \left. + (\sin \alpha x_m) J_1\left(\alpha\left(\frac{w}{2}-x_m\right)\right)\right\} \\ & - \frac{\nu(\nu-1)x_m}{(\alpha x_m)^{\nu+1}}\{(\cos \alpha x_m) \\ & \cdot (S(0,\nu-1) - S(\alpha x_m, \nu-1)) \\ & - (\sin \alpha x_m)(C(0,\nu-1) \\ & \left. - C(\alpha x_m, \nu-1))\}\Bigg] \end{aligned} \tag{8a}$$

$$\begin{aligned} \tilde{I}_{z1}(\alpha) = & \frac{2}{\alpha}\sin\frac{\alpha w}{2} + \frac{10\left(1-\frac{2x_c}{w}\right)}{M(x_c)-1} \\ & \cdot\left\{\frac{\pi w}{2} J_0\left(\frac{|\alpha| w}{2}\right) - \frac{2}{\alpha}\sin\frac{\alpha w}{2}\right\} \end{aligned} \tag{8b}$$

and $H_1(z)$ is a Struve function [9, p. 496, eq. (12.1.6)], $J_i(z)$ is a ith order Bessel function [9, p. 360, eq. (9.1.20)], and $C(x, a)$ and $S(x, a)$ are incomplete gamma functions [9, p. 262, eqs. (6.5.7) and (6.5.8)].

Then, we can obtain the integral simultaneous equations to solve for β according to [4] as follows:

$$K11 c_1 + K12 d_1 = 0 \tag{9a}$$

$$K21 c_1 + K22 d_1 = 0 \tag{9b}$$

where

$$K11 = 2\int_0^{\infty} \tilde{I}_{z1}(\alpha) G_{11} \tilde{I}_{x1}(\alpha)\, d\alpha \tag{10a}$$

$$K12 = 2\int_0^{\infty} \tilde{I}_{z1}(\alpha) G_{12} \tilde{I}_{z1}(\alpha)\, d\alpha \tag{10b}$$

$$K21 = 2\int_0^{\infty} \tilde{I}_{x1}(\alpha) G_{21} \tilde{I}_{x1}(\alpha)\, d\alpha \tag{10c}$$

$$K22 = 2\int_0^{\infty} \tilde{I}_{x1}(\alpha) G_{22} \tilde{I}_{z1}(\alpha)\, d\alpha \tag{10d}$$

and the G_{ij} are given in [4], following the corrections mentioned above. Now, we can obtain β as the root of the following determinant:

$$\text{Det} = K11K22 - K12K21 = 0. \tag{11}$$

The propagation constant $\beta(f)$ at an operating frequency f can be expressed as follows:

$$\beta(f) = k_0\sqrt{\epsilon^*_{\text{eff}}(f)} \tag{12}$$

where $k_0 (= \omega/v_0$, $v_0 =$ velocity of light in free space) denotes the propagation constant in free space and $\epsilon^*_{\text{eff}}(f)$ the effective relative permittivity at the frequency f. Therefore, calculation of β is identical to calculating $\epsilon^*_{\text{eff}}(f)$.

The numerical calculations of the integrations in (10) are actually performed from zero to an upper limit α_U with

TABLE I
COMPARISON BETWEEN THE METHOD OF INVERSE INTERPOLATION AND THE PRESENT METHOD

METHOD	ACCU	TN	h/λ_0 = 0.005	0.20	0.40
A	10^{-3}	28	5.46762	7.36375	7.75010
	10^{-5}	56	5.46732	7.35960	7.74748
B	10^{-3}	7	5.46730	7.35928	7.74745

$\epsilon^* = 8$, $w/h = 1$
A: METHOD OF INVERSE INTERPOLATION
B: PRESENT METHOD
ACCU: ACCURACY OF NUMERICAL INTEGRATIONS(10)
TN: TOTAL NUMBER OF NUMERICAL INTEGRATIONS

TABLE II
COMPARISON BETWEEN THE ITERATION METHOD AND THE PRESENT METHOD

	ITERATION METHOD	PRESENT METHOD	
		B	C
$\epsilon^*_{eff}(f)$	6.51912	6.51941	6.51914

$\epsilon^* = 9.7$, $h = 1.27$ mm, $w = 1.219$ mm, $f = 1$ GHz
B: PRESENT METHOD USING BOTH $I_z(x)$ AND $I_x(x)$
C: PRESENT METHOD USING ONLY $I_z(x)$
ITERATION METHOD: FUJIKI et al.[2, table 1]

respect to an integral variable α due to limits on computation time. We take $\alpha_U = 3\times10^3/w$ in the present paper.

On the other hand, we can understand easily that it takes more computation time to obtain $\epsilon^*_{eff}(f)$ by the method of inverse interpolation using two initial trial values of $\epsilon^*_{eff}(f)$, because each numerical calculation time of $K11$, $K12$, $K21$, and $K22$ of (10) is intrinsically long and because these calculations must be performed for each successive trial value ϵ^*_{eff}.

Now $K11$, $K21$, and $K22$ are only weakly dependent on the trial value ϵ^*_{eff}, but $K12$ depends strongly and almost linearly on it. These characteristics lead to an effective method of calculation (see the Appendix for details). Using this method, we can seek $\epsilon^*_{eff}(f)$ accurately and automatically by using only the initial trial value $\epsilon^*_{eff}(①)$. The other advantage of this method is that $\epsilon^*_{eff}(①)$ can be obtained using the approximate formulas for $\epsilon^*_{eff}(f)$ proposed already [6], [11], [12],[2] although two initial trial values that satisfy Det < 0 and Det > 0, respectively, must be given in the method of inverse interpolation. In this paper, $\epsilon^*_{eff}(①)$ is obtained using formula YK given in [12].

III. EFFECTIVE RELATIVE PERMITTIVITY $\epsilon^*_{eff}(f)$

Table I shows the comparison between the results obtained by the method of inverse interpolation (method A) and the present one (method B). For method A, the results are shown for two cases where the numerical calculations of the integrations shown in (10) are accurate to better than 10^{-3} and 10^{-5}, respectively. The total number (TN) of numerical integrations is also shown in Table I. The computation time is almost proportional to TN. The present method (B) reduces the computation time by a factor of about five compared with method A. An agree-

[2]Main misprints in [12]: $m(\epsilon^*_\xi, \epsilon^*_\eta, \pi/2-\gamma) \rightarrow \{m(\epsilon^*_\xi, \epsilon^*_\eta, \pi/2-\gamma)\}^2$ in (6); $4\pi h \rightarrow 4h$ in (9); $\sqrt{\epsilon^*_\parallel \epsilon^*_\perp}/2$ (= about 5.221) $\rightarrow (\sqrt{\epsilon^*_\parallel \epsilon^*_\perp}+1)/2$ (= about 5.721) below fig. 2.

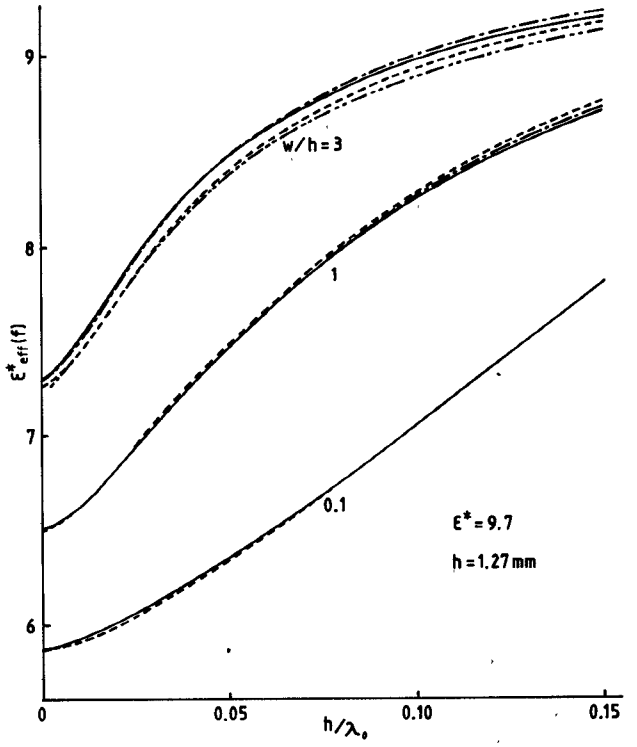

Fig. 2. Comparison of $\epsilon^*_{eff}(f)$. $\epsilon^* = 9.7$, $h = 1.27$ mm. —— present method using both $I_z(x)$ and $I_x(x)$. — - — present method using only $I_z(x)$. — — — present method using only $I_z(x)$ where $I_z(x) = M(x)$. ----- Kowalski and Pregla [3].

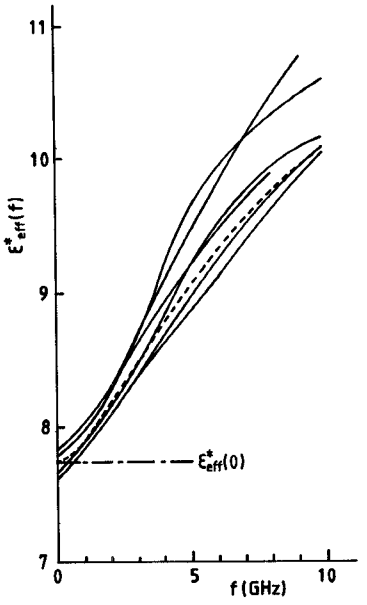

Fig. 3. Comparison of $\epsilon^*_{eff}(f)$ computed by various authors. $\epsilon^* = 11.7$, $w/h = 0.96$, $h = 3.17$ mm. —— various results illustrated in Kuester and Chang [5, fig. 2]. ----- present method. — - — $\epsilon^*_{eff}(0)$ by Green's function technique [10].

TABLE III
EFFECTIVE RELATIVE PERMITTIVITY $\epsilon^*_{eff}(f)$

ϵ^*	w/h \ h/λ_0	0	0.005	0.05	0.1	0.2	0.3	0.4	0.7	1.0
2	0.4	1.60329	1.604	1.629	1.667	1.740	1.800	1.846	1.922	1.960
	1	1.64667	1.648	1.682	1.728	1.806	1.859	1.893	1.945	1.966
	2	1.69807	1.700	1.743	1.795	1.867	1.907	1.930	1.963	1.976
4	0.4	2.78862	2.793	2.926	3.106	3.413	3.614	3.737	3.905	3.944
	1	2.91642	2.923	3.105	3.317	3.595	3.737	3.814	3.916	3.953
	2	3.07119	3.081	3.311	3.523	3.734	3.825	3.875	3.940	3.965
8	0.1	4.92578	4.937	5.270	5.765	6.799	7.367	7.633	7.876	7.939
	0.4	5.14550	5.163	5.650	6.241	7.067	7.472	7.671	7.881	7.940
	1	5.44034	5.468	6.124	6.742	7.361	7.620	7.747	7.898	7.945
	2	5.80203	5.844	6.633	7.158	7.574	7.739	7.823	7.924	7.956
	10	6.88677	7.020	7.597	7.768	7.884	7.926	7.948	7.974	7.984
16	0.4	9.85123	9.917	11.48	13.11	14.79	15.42	15.65	15.88	15.94
	1	10.4789	10.58	12.59	14.01	15.13	15.52	15.70	15.89	15.94
	2	11.2545	11.41	13.63	14.68	15.40	15.66	15.78	15.91	15.95
128	0.4	75.6653	78.38	111.3	122.4	126.5	127.3	127.6	127.9	127.9
	1	80.9729	85.03	116.4	123.6	126.6	127.3	127.6	127.9	127.9
	2	87.5449	93.56	120.3	124.9	127.0	127.5	127.7	127.9	127.9
ϵ^*	w/h \ h/λ_0	0	1×10^{-7}	1×10^{-6}	1×10^{-5}	1×10^{-4}	0.001	0.002	0.003	0.004
8	1	5.44034	5.4406	5.4406	5.4406	5.4406	5.4424	5.4464	5.4521	5.4592

$f = (v_0/h)/(h/\lambda_0)$. $\epsilon^*_{eff}(0)[= 1 + \epsilon^*(1 - q)]$ was calculated by using effective filling fraction q[10, table I].

ment of four to five significant digits is seen between the results of the two methods.

Table II compares the results obtained here with those obtained through the iteration method proposed by Fujiki *et al.* [2]. The result of [2] is the value for the case when the total number of basis functions in (4) was taken as $M + N = 20$. An agreement of four significant digits is seen between the results of the two methods. Table II also includes results obtained by using only the longitudinal current distribution $I_z(x)$. For this case, we can seek $\epsilon^*_{eff}(f)$ as the value satisfying $K12 = 0$. We find that this result also has four significant digits, confirming that $I_z(x)$ of (5b) is expressed in accurate closed form for the longitudinal current distribution.

Fig. 2 shows a comparison of the effective relative permittivities $\epsilon^*_{eff}(f)$ computed by the present method and the method outlined by Kowalski and Pregla [3]. We could confirm that the results by the present method using both $I_x(x)$ and $I_z(x)$ or only $I_z(x)$ accurately approach the exact values of $\epsilon^*_{eff}(0)$ calculated by the Green's function technique [10]: $\epsilon^*_{eff}(0) = 7.28922$ for $w/h = 3$, 6.51149 for $w/h = 1$, and 5.87415 for $w/h = 0.1$. In addition, the curves of $\epsilon^*_{eff}(f)$ for both cases are in good agreement and cannot be distinguished from each other for $w/h = 0.1$. On the other hand, the curves of Kowalski and Pregla [3] are in agreement with those of the present method for the smaller shape ratio but are in disagreement for $w/h = 3$. Additionally, the result of [3] for $w/h = 3$ differs at $f = 0$ from the exact value of $\epsilon^*_{eff}(0)$, and this difference continues at higher frequencies.

To explain this discrepancy, one extra curve for $w/h = 3$ is given in Fig. 2 for $\epsilon^*_{eff}(f)$ computed by the present method using only $I_z(x) = M(x)$, where $M(x)$ is the Maxwell distribution shown in (6). This $M(x)$ is different from the $I_z(x)$ shown in (5b) for w/h larger than 0.7, as illustrated in [13, fig. 4].

From a comparison of the various curves in Fig. 2, we can conclude that $I_z(x)$ determines the major magnitude of $\epsilon^*_{eff}(f)$ and that $I_x(x)$ acts as the adjuster of its magnitude. On the other hand, Kuester and Chang [5] already suggested that inaccurate expressions for $I_z(x)$ and $I_x(x)$ cause important discrepancies between the various results. This can be confirmed in Fig. 2 and also from the comparison in Fig. 3, in which the curve of $\epsilon^*_{eff}(f)$ obtained by the present method is shown together with the various curves given in [5].

Table III presents the results of $\epsilon^*_{eff}(f)$ computed by the present method and also shows good convergence to the exact value $\epsilon^*_{eff}(0) = 5.44034$ in the case of $\epsilon^* = 8$ and $w/h = 1$.

IV. CONCLUSIONS

It has been shown that the method described here can compute $\epsilon^*_{eff}(f)$ effectively and automatically with great savings in computation time. The numerical results shown in the tables and figures are believed to be obtained with a high degree of accuracy and thus can be used as reference standards. It has been confirmed that $I_z(x)$ determines the major magnitude of $\epsilon^*_{eff}(f)$ and that $I_x(x)$ acts as the adjuster of its magnitude.

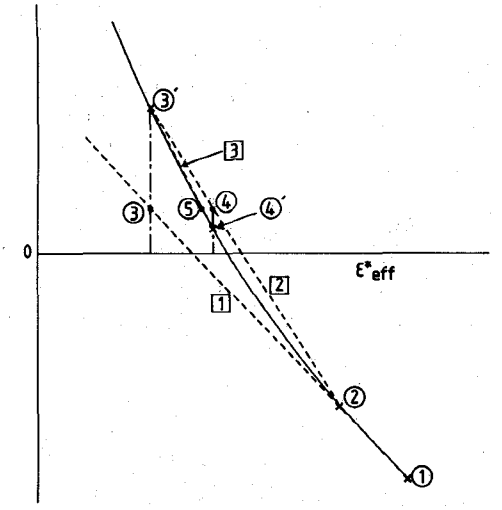

Fig. 4. Diagram of the method for effectively calculating ϵ^*_{eff}.

APPENDIX

We first obtain the trial value $\epsilon^*_{eff}(①)$ and calculate $K11$, $K12$, $K21$, and $K22$ for this value. As explained in Section II, the values of $K11$, $K21$, and $K22$ are constant, even if we change the trial value ϵ^*_{eff}. Therefore, we can estimate $K12$ satisfying Det = 0 shown in (11) by using $K11(①)$, $K21(①)$, and $K22(①)$ obtained above and denoting its value as $K12$(app). This $K12$(app) is the value of $K12$ corresponding to the $\epsilon^*_{eff}(f)$ to be sought. Fig. 4 illustrates the procedure, starting from the initial point ① and seeking the final point ⑤ having the value of $K12$(app) on the curve of $K12$ (solid line). The second trial value $\epsilon^*_{eff}(②)$ is given with the value shifted by 0.1 percent from $\epsilon^*_{eff}(①)$ in this paper. The $\epsilon^*_{eff}(⑤)$ for the point ⑤ in Fig. 4 is the final value.

ACKNOWLEDGMENT

The authors would like to thank the reviewers for their valuable advice and for the reference to [9].

REFERENCES

[1] E. J. Denlinger, "A frequency dependent solution for microstrip transmission lines," *IEEE Trans. Microwave Theory Tech.*, vol. MTT-19, pp. 30–39, Jan. 1971.

[2] Y. Fujiki, Y. Hayashi, and M. Suzuki, "Analysis of strip transmission lines by iteration method," *J. Inst. Electron. Commun. Eng. Japan*, vol. 55-B, pp. 212–219, May 1972 (in Japanese); *Electron. Commun. Japan*, vol. 55, pp. 74–80, May 1972.

[3] G. Kowalski and R. Pregla, "Dispersion characteristics of single and coupled microstrips," *Arch. Elek. Übertragungstech.*, vol. 26, pp. 276–280, June 1972.

[4] T. Itoh and R. Mittra, "Spectral-domain approach for calculating the dispersion characteristics of microstrip lines," *IEEE Trans. Microwave Theory Tech.*, vol. MTT-21, pp. 496–499, July 1973.

[5] E. F. Kuester and D. C. Chang, "An appraisal of methods for computation of the dispersion characteristics of open microstrip," *IEEE Trans. Microwave Theory Tech.*, vol. MTT-27, pp. 691–694, July 1979.

[6] E. Yamashita, K. Atsuki, and T. Ueda, "An approximate dispersion formula of microstrip lines for computer-aided design of microwave integrated circuits," *IEEE Trans. Microwave Theory Tech.*, vol. MTT-27, pp. 1036–1038, Dec. 1979.

[7] M. Hashimoto, "A rigorous solution for dispersive microstrip," *IEEE Trans. Microwave Theory Tech.*, vol. MTT-33, pp. 1131–1137, Nov. 1985.

[8] R. Mittra and S. W. Lee, *Analytical Techniques in the Theory of Guided Waves*. New York: Macmillan, 1971, pp. 4–11.

[9] M. Abramowitz and I. A. Stegun, *Handbook of Mathematical Functions with Formulas, Graphs, and Mathematical Tables*. New York: Dover, 1964.

[10] M. Kobayashi, "Analysis of the microstrip and the electrooptic light modulators," *IEEE Trans. Microwave Theory Tech.*, vol. MTT-26, pp. 119–126, Feb. 1978.

[11] M. Kobayashi, "Important role of inflection frequency in the dispersive property of microstrip lines," *IEEE Trans. Microwave Theory Tech.*, vol. MTT-30, pp. 2057–2059, Nov. 1982.

[12] M. Kobayashi, "Frequency dependent characteristics of microstrip on anisotropic substrates," *IEEE Trans. Microwave Theory Tech.*, vol. MTT-30, pp. 2054–2057, Nov. 1982.

[13] M. Kobayashi, "Longitudinal and transverse current distributions on microstriplines and their closed-form expression," *IEEE Trans. Microwave Theory Tech.*, vol. MTT-33, pp. 784–788, Sept. 1985.

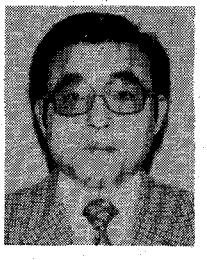

Masanori Kobayashi (M'79) was born in Niigata, Japan, on June 17, 1947. He received the B.E. and M.E. degrees in electrical engineering from Ibaraki University, Ibaraki, Japan, in 1970 and 1972, respectively, and the D.E. degree in electrical and electronic engineering from the Tokyo Institute of Technology in 1981.

Since April 1972, he has been with the Department of Electrical Engineering at Ibaraki University. He was a Research Assistant from April 1972 to March 1981 and a Lecturer from April 1981 to July 1982. Since August 1982, he has been an Associate Professor. His research interests are in microstrip transmission lines, dielectric optical waveguides, magnetic elements, and relativistic electromagnetic theory.

Dr. Kobayashi is a member of the Institute of Electrical Engineers of Japan and the Institute of Electronics and Communication Engineers of Japan.

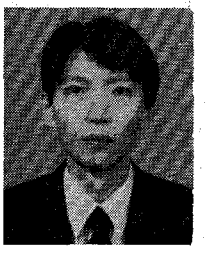

Fumihiro Ando was born in Fukushima, Japan, on January 25, 1962. He received the B.E. and M.E. degrees in electrical engineering from Ibaraki University, Ibaraki, Japan, in 1984 and 1986, respectively.

In April 1986, he joined Korg Inc., Tokyo, Japan, where he is currently engaged in research on acoustic devices.

Mr. Ando is a member of the Institute of Electronics and Communication Engineers of Japan.